



**AMS**  
American Meteorological Society

## Supplemental Material

*Journal of Climate*

Storm Size Modulates Tropical Cyclone Intensification through an Oceanic Pathway in Global Oceans

<https://doi.org/10.1175/JCLI-D-24-0398.1>

[Copyright 2025 American Meteorological Society](#) (AMS)

For permission to reuse any portion of this work, please contact [permissions@ametsoc.org](mailto:permissions@ametsoc.org). Any use of material in this work that is determined to be “fair use” under Section 107 of the U.S. Copyright Act (17 USC §107) or that satisfies the conditions specified in Section 108 of the U.S. Copyright Act (17 USC §108) does not require AMS’s permission. Republication, systematic reproduction, posting in electronic form, such as on a website or in a searchable database, or other uses of this material, except as exempted by the above statement, requires written permission or a license from AMS. All AMS journals and monograph publications are registered with the Copyright Clearance Center (<https://www.copyright.com>). Additional details are provided in the AMS Copyright Policy statement, available on the AMS website (<https://www.ametsoc.org/PUBSCopyrightPolicy>).

**Supplementary materials for**  
**“Storm Size Modulates Tropical Cyclone Intensification Through an**  
**Oceanic Pathway in global ocean basins”**

Yuhao Liu<sup>a</sup>, Shoude Guan<sup>a,b,c</sup>, I-I Lin<sup>d</sup>, Wei Zhao<sup>a,b,c</sup>, Fei-Fei Jin<sup>f</sup>, Ping Liu<sup>a</sup>, Jiwei  
Tian<sup>a,b,c</sup>

<sup>a</sup> *Frontier Science Center for Deep Ocean Multispheres and Earth System (FDOMES) and  
Physical Oceanography Laboratory/Key Laboratory of Ocean Observation and Information of Hainan  
Province, Sanya Oceanographic Institution, Ocean University of China, Qingdao/Sanya, China.*

<sup>b</sup> *SANYA Oceanographic Laboratory, Sanya, China.*

<sup>c</sup> *Laboratory for Ocean Dynamics and Climate, Qingdao Marine Science and Technology Center,  
Qingdao, China.*

<sup>d</sup> *Department of Atmospheric Sciences, National Taiwan University, Taipei, Taiwan.*

<sup>e</sup> *Department of Atmospheric Sciences, SOEST, University of Hawaii at Manoa, Honolulu, Hawaii,  
USA.*

*Corresponding author: Shoude Guan (guanshoude@ouc.edu.cn)*

## **Description of the material**

Figure S1: Scatterplots of the SSTA versus  $V_{max}$  using all TC track-points in global oceans.

Figure S2: Spatial patterns of composited SSTA for different R34 groups associated with Tropical Storms (TS) in different TC-active basins.

Figure S3: Spatial patterns of composited SSTA for different R34 groups associated with Categories 3–5 (Cat 3–5) TCs in different TC-active basins.

Figure S4: Scatterplots of the TC-induced SSTA, enthalpy flux, and TC IR against the R34 of per 25th percentiles for TS in different TC-active basins.

Figure S5: Scatterplots of the TC-induced SSTA, enthalpy flux, and TC IR against the R34 of per 25th percentiles for Cat 3–5 TCs in different TC-active basins.

Figure S6: Spatial patterns of composited SSTA associated with non-RI and RI cases for TS in different TC-active basins.

Figure S7: Spatial patterns of composited SSTA associated with non-RI and RI cases for Cat 3–5 TCs in different TC-active basins.

Figure S8: Assessment of the role of R34,  $U_h$  and  $dT$  in TC-induced SSTA for TS in different TC-active basins.

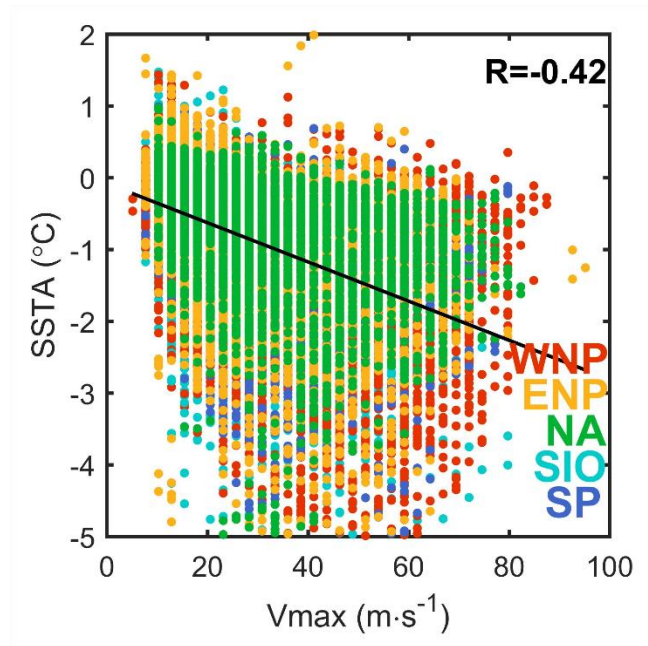
Figure S9: Assessment of the role of R34,  $U_h$  and  $dT$  in TC-induced SSTA for Cat 3–5 in different TC-active basins.

Table S1: Statistics of the composited TC-induced SSTA for different R34 groups associated with TS in different TC-active basins.

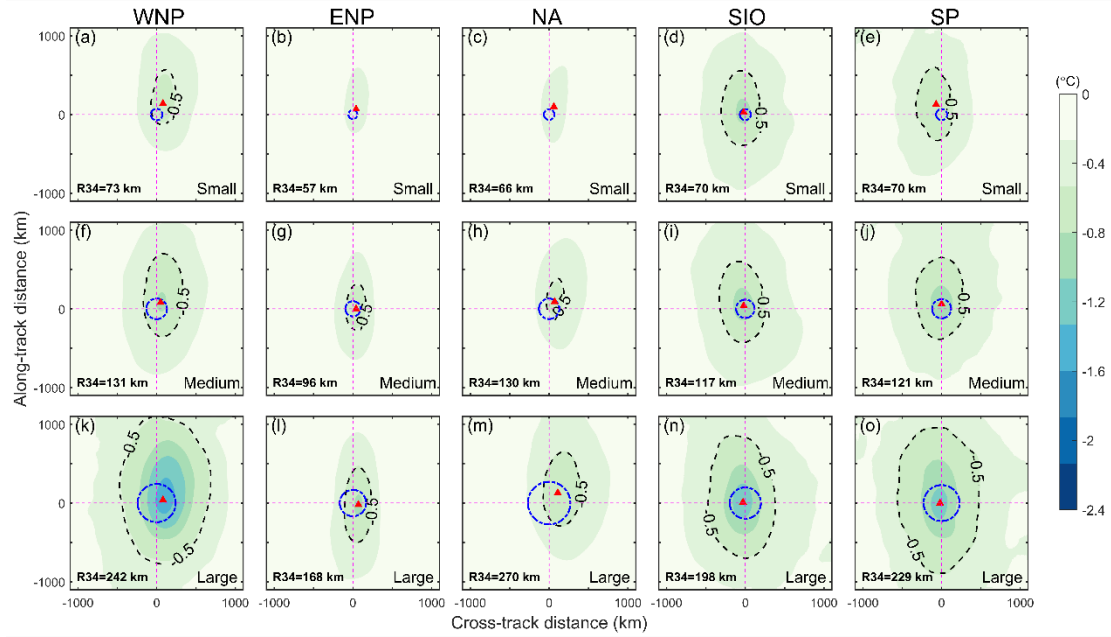
Table S2: Statistics of the composited TC-induced SSTA for different R34 groups associated with Cat 3–5 TCs in different TC-active basins.

Table S3: Statistics of the composited TC-induced SSTA for non-RI and RI cases for TS in different TC-active basins.

Table S4: Statistics of the composited TC-induced SSTA for non-RI and RI cases for Cat 3–5 TCs in different TC-active basins.



**Figure S1.** Scatterplots of the SSTA versus Vmax using all TC track-points in global oceans.



**Figure S2.** Same as Fig. 4, but for tropical storms (TS). Spatial patterns of composited SSTA associated with TS in different TC-active basins (from left to right, WNP, ENP, NA, SIO, and SP). (a–e) composited SSTA for TCs with R34 smaller than 25th percentiles in each basin; (f–j) as in (a–e), but for medium TCs with R34 between 25th and 75th percentiles in each basin; (k–o) as in (a), but for large TCs with R34 larger than 75th percentiles in each basin; The blue dotted-dashed circle in each figure indicates the average R34. The black dashed line in each figure indicates the contour of SSTA=-0.5 °C. The red triangle in each figure indicates the location of the maximum TC-induced SSTA. The average R34 is shown in the lower-left corner in each figure.

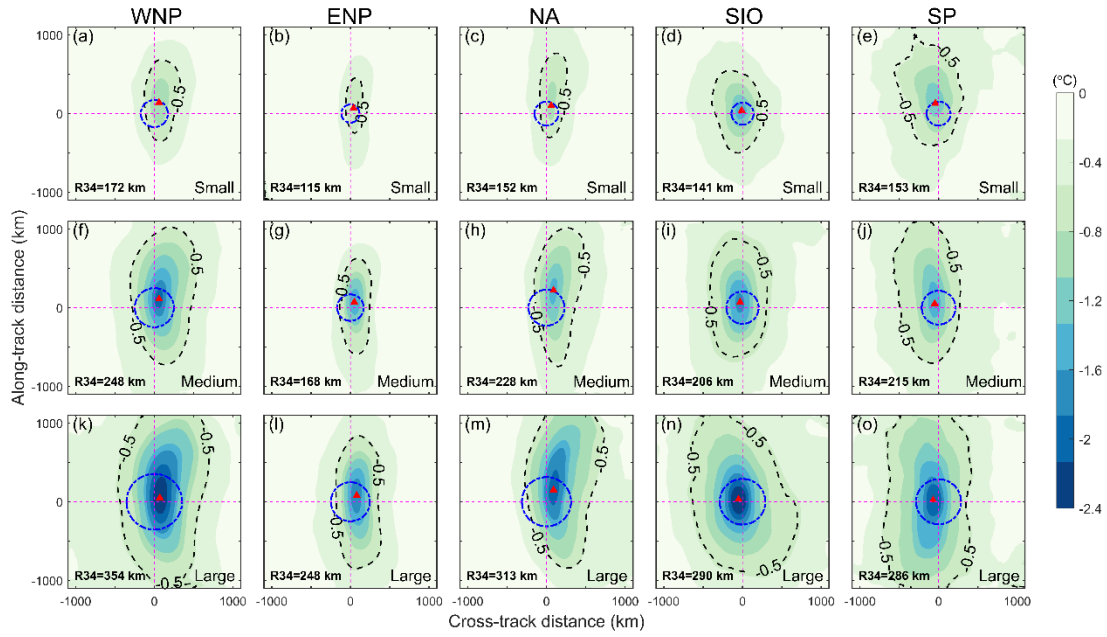


**Figure S3.** Same as Fig. 4, but for Cat 3–5 TCs. Spatial patterns of composited SSTA associated with Cat 3–5 TCs in different TC-active basins (from left to right, WNP, ENP, NA, SIO, and SP). (a–e) composited SSTA for TCs with R34 smaller than 25th percentiles in each basin; (f–j) as in (a–e), but for medium TCs with R34 between 25th and 75th percentiles in each basin; (k–o) as in (a), but for large TCs with R34 larger than 75th percentiles in each basin; The blue dotted-dashed circle in each figure indicates the average R34. The black dashed line in each figure indicates the contour of SSTA=-0.5 °C. The red triangle in each figure indicates the location of the maximum TC-induced SSTA. The average R34 is shown in the lower-left corner in each figure.

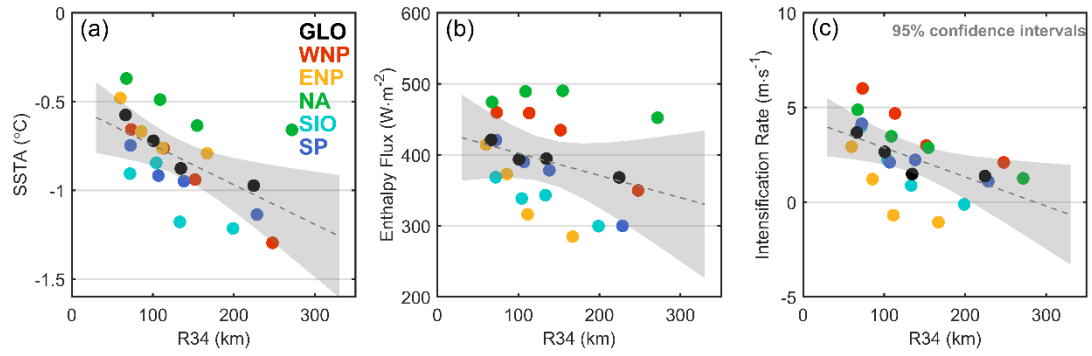


**Figure S4.** Same as Fig. 9, but for TS. Scatterplots of the (a) TC-induced SSTA, (b) enthalpy flux, and (c) TC IR against the R34 for TS in all TC-active basins. Linear regression trend lines in SSTA, enthalpy flux and TC IR with R34 are shown as gray dashed lines, and the gray shaded areas indicate the 95% confidence intervals.

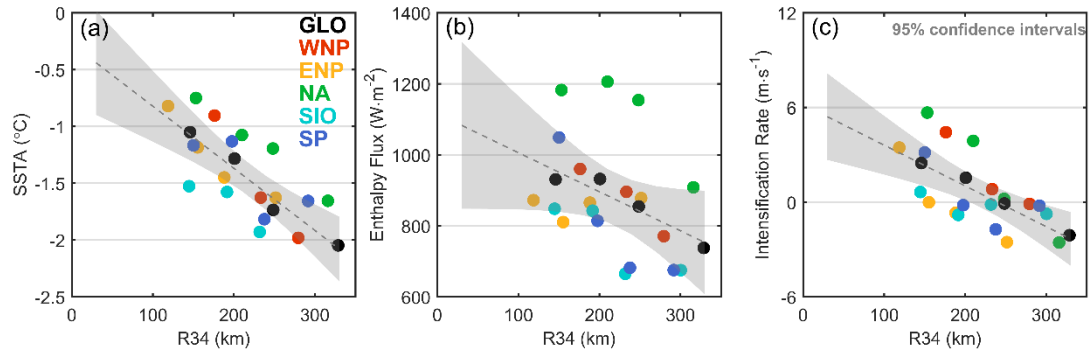


**Figure S5.** Same as Fig. 9, but for Cat 3–5 TCs. Scatterplots of the (a) TC-induced SSTA, (b) enthalpy flux, and (c) TC IR against the R34 for Cat 3–5 TCs in all TC-active basins. Linear regression trend lines in SSTA, enthalpy flux and TC IR with R34 are shown as gray dashed lines, and the gray shaded areas indicate the 95% confidence intervals.



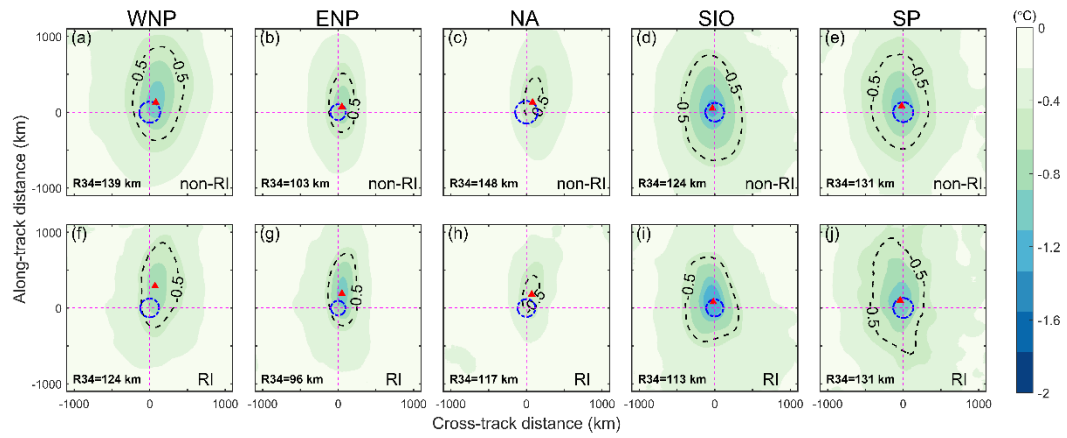


**Figure S6.** Same as [Fig. 10](#), but for the composited SSTA with (a–e) non-RI and (f–j) RI TS.

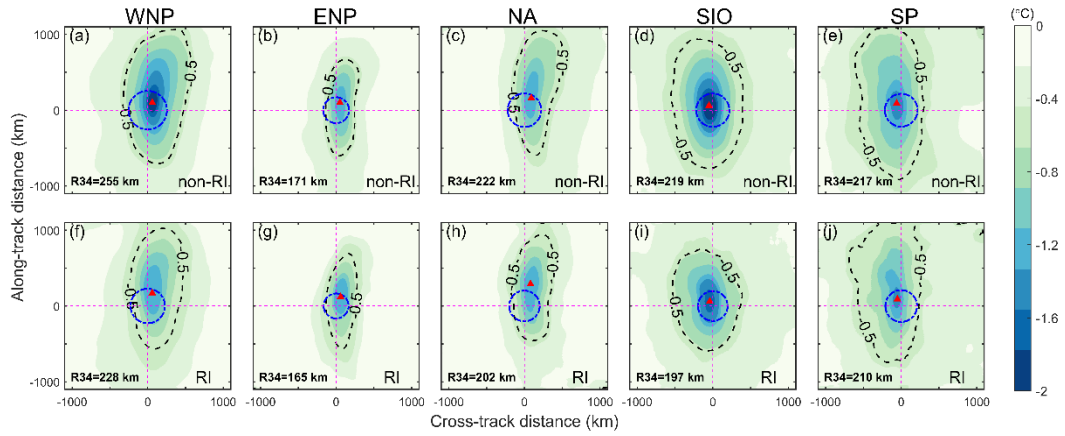


**Figure S7.** Same as [Fig. 10](#), but for the composited SSTA with (a–e) non-RI and (f–j) RI Cat 3–5 TCs.

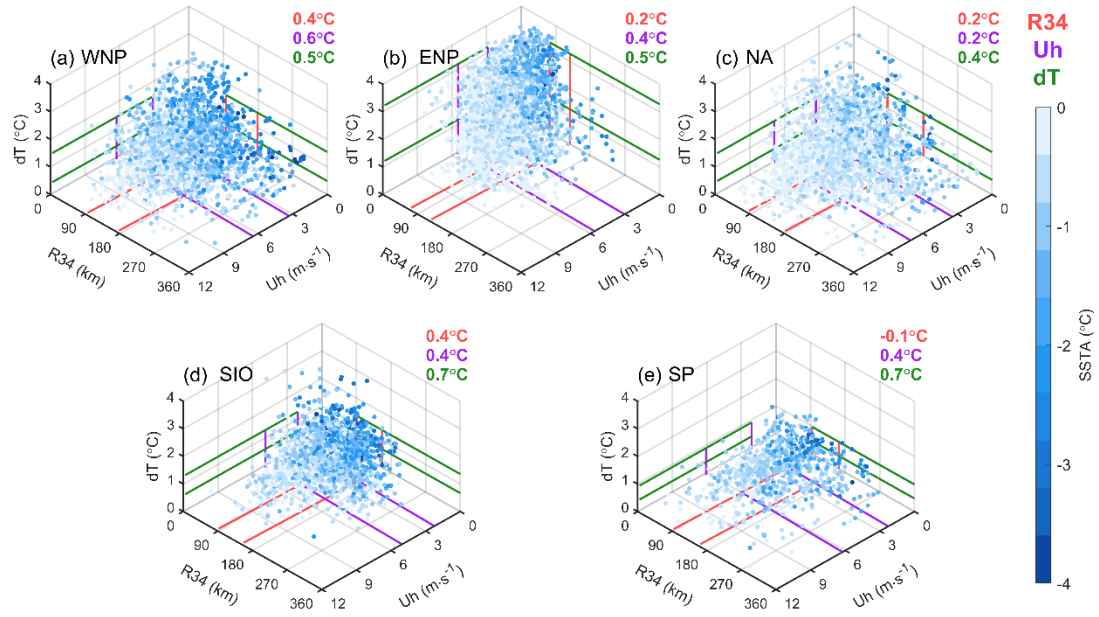


**Figure S8.** Same as Fig. 13, but for TS. Assessment of the role of R34, Uh and dT in TC-induced SSTA for TS in different basins. Scatterplots of the SSTA versus R34 (y-axis), Uh (x-axis) and dT (z-axis) for TCs in the (a) WNP, (b) ENP, (c) NA, (d) SIO and (e) SP. The red, violet and green solid lines in each figure indicate the 25th and 75th percentiles of R34, Uh and dT, respectively. The colored texts in the upper-right corner represent the SSTA difference induced by small, fast TCs with weak stratification and large, slow TCs with strong stratification.

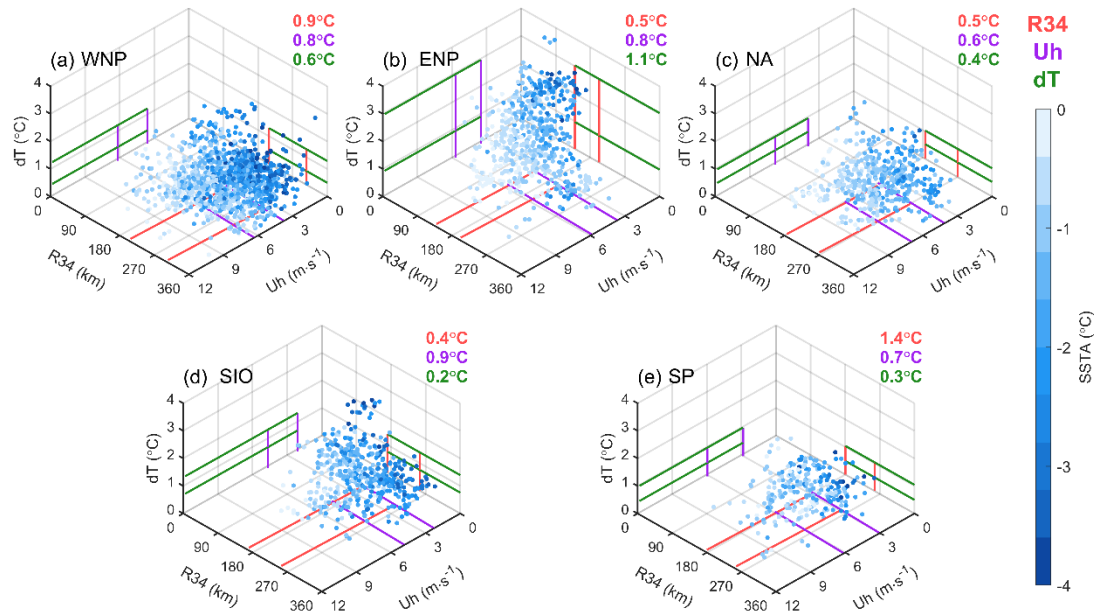


**Figure S9.** Same as Fig. 13, but for Cat 3–5 TCs. Assessment of the role of R34, Uh and dT in TC-induced SSTA for Cat 3–5 in different basins. Scatterplots of the SSTA versus R34 (y-axis), Uh (x-axis) and dT (z-axis) for TCs in the (a) WNP, (b) ENP, (c) NA, (d) SIO and (e) SP. The red, violet and green solid lines in each figure indicate the 25th and 75th percentiles of R34, Uh and dT, respectively. The colored texts in the upper-right corner represent the SSTA difference induced by small, fast TCs with weak stratification and large, slow TCs with strong stratification.

**Table S1.** Same as [Table 2](#), but for TS. Statistics of the composited TC-induced SSTA for different R34 groups associated with TS in different TC-active basins.

		WNP	ENP	NA	SIO	SP
R34 (km)	Small	73±1.2	57±0.7	66±1.1	70±1.4	70±2.0
	Medium	131±1.1	96±0.7	130±1.4	117±1.0	121±1.6
	Large	242±4.4	168±2.7	270±7.4	198±3.1	229±6.1
Uh (m s <sup>-1</sup> )	Small	4.9±0.2	4.5±0.1	5.4±0.2	3.8±0.2	4.6±0.4
	Medium	5.1±0.1	4.3±0.1	5.3±0.1	3.8±0.1	4.2±0.2
	Large	5.2±0.2	4.6±0.1	5.3±0.2	4.1±0.2	5.1±0.4
RT (hour)	Small	11.4±0.7	9.5±0.6	9.9±0.9	14.1±1.4	13.0±1.3
	Medium	19.5±0.8	16.6±0.7	19.9±1.1	26.3±1.4	25.9±2.1
	Large	36.2±2.3	25.0±1.3	42.1±4.4	38.0±2.7	47.6±7.3
SSTA within 100 km (°C)	Small	-0.5	-0.4	-0.3	-0.8	-0.6
	Medium	-0.7	-0.6	-0.5	-0.9	-0.9
	Large	-1.3	-0.7	-0.6	-1.1	-1.1
Maximum SSTA (°C)	Small	-0.7	-0.4	-0.4	-0.9	-0.7
	Medium	-0.8	-0.7	-0.6	-1.1	-0.9
	Large	-1.4	-0.8	-0.7	-1.2	-1.1
Cold wake area (×10 <sup>4</sup> km <sup>2</sup> )	Small	17.1	/	/	39.0	32.8
	Medium	41.6	11.8	8.6	47.4	51.5
	Large	168.5	26.0	35.1	104.7	150.2
Shift (km)	Small	50	40	60	-20	-20
	Medium	50	70	70	-20	-30
	Large	80	70	110	-30	-70

**Table S2.** Same as [Table 2](#), but for Cat 3–5 TCs. Statistics of the composited TC-induced SSTA for different R34 groups associated with Cat 3–5 TCs in different TC-active basins.

		WNP	ENP	NA	SIO	SP
R34 (km)	Small	172±2.4	115±2.4	152±2.7	141±2.7	153±2.8
	Medium	248±1.9	168±2.0	228±2.6	206±2.6	215±2.6
	Large	354±5.2	248±5.1	313±8.3	290±4.6	286±4.0
Uh (m s <sup>-1</sup> )	Small	5.6±0.2	4.9±0.3	5.6±0.3	3.1±0.2	4.1±0.2
	Medium	5.1±0.1	4.7±0.2	5.5±0.2	3.9±0.2	4.8±0.3
	Large	5.1±0.2	4.9±0.2	5.4±0.3	4.0±0.3	5.8±0.5
RT (hour)	Small	21.8±1.6	16.5±1.7	17.6±1.1	33.2±2.9	24.7±1.6
	Medium	35.8±2.3	22.9±1.5	29.0±2.7	38.3±3.0	31.9±2.7
	Large	46.1±2.8	31.0±1.4	38.1±2.7	55.8±5.0	44.5±5.4
SSTA within 100 km (°C)	Small	-0.8	-0.6	-0.7	-1.3	-1.0
	Medium	-1.6	-1.2	-1.0	-1.5	-1.2
	Large	-2.1	-1.4	-1.5	-2.1	-1.8
Maximum SSTA (°C)	Small	-1.0	-0.7	-0.8	-1.5	-1.3
	Medium	-1.9	-1.4	-1.4	-1.7	-1.4
	Large	-2.5	-1.8	-2.0	-2.4	-2.1
Cold wake area (×10 <sup>4</sup> km <sup>2</sup> )	Small	35.3	12.2	28.8	50.1	80.7
	Medium	114.0	39.1	78.2	90.2	115.9
	Large	208.1	80.7	143.9	199.7	216.1
Shift (km)	Small	60	40	60	-10	-40
	Medium	60	50	90	-30	-50
	Large	70	80	90	-50	-70

**Table S3.** Same as [Table 3](#), but for TS. Statistics of the composited TC-induced SSTA for non-RI and RI cases for TS in different TC-active basins.

		WNP	ENP	NA	SIO	SP
R34 (km)	Non-RI	139±3.2	103±2.4	148±4.6	124±3.2	131±5.2
	RI	124±6.6	96±5.0	117±8.5	113±5.7	131±9.8
Uh (m s <sup>-1</sup> )	Non-RI	4.9±0.1	4.4±0.1	5.4±0.1	3.9±0.1	4.4±0.2
	RI	5.2±0.3	5.0±0.2	5.5±0.3	3.5±0.3	4.6±0.4
RT (hour)	Non-RI	21.2±1.0	16.8±0.8	22.4±1.8	25.7±1.6	28.3±3.3
	RI	17.2±2.0	12.4±0.9	13.9±1.3	25.2±3.0	23.3±2.6
SSTA within 100 km (°C)	Non-RI	-0.8	-0.7	-0.5	-1.2	-0.9
	RI	-0.6	-0.6	-0.5	-1.1	-0.9
Cold wake area (×10 <sup>4</sup> km <sup>2</sup> )	Non-RI	64.6	28.9	11.0	85.2	79.7
	RI	41.5	20.7	9.9	60.9	73.1

**Table S4.** Same as [Table 3](#), but for Cat 3–5 TCs. Statistics of the composited TC-induced SSTA for non-RI and RI cases for Cat 3–5 TCs in different TC-active basins.

		WNP	ENP	NA	SIO	SP
R34 (km)	Non-RI	255±7.5	171±6.6	222±8.1	219±7.7	217±6.6
	RI	228±6.4	165±6.5	202±7.9	197±7.3	210±8.0
Uh (m s <sup>-1</sup> )	Non-RI	5.1±0.2	4.8±0.2	5.6±0.3	3.8±0.3	4.5±0.3
	RI	5.3±0.2	5.0±0.2	5.7±0.2	3.5±0.2	4.5±0.3
RT (hour)	Non-RI	35.1±2.6	22.6±1.6	25.1±1.7	42.3±3.7	34.7±3.4
	RI	28.8±2.0	21.0±1.6	22.1±1.2	38.0±3.0	34.6±3.4
SSTA within 100 km (°C)	Non-RI	-1.5	-1.0	-1.0	-1.7	-1.3
	RI	-1.0	-0.9	-0.9	-1.4	-1.1
Cold wake area (×10 <sup>4</sup> km <sup>2</sup> )	Non-RI	118.5	43.0	74.2	128.8	141.5
	RI	87.3	37.0	60.7	90.7	131.6